

STUDY ON THE RESPONSE OF ELASTOMERIC BEARINGS WITH 3D NUMERICAL SIMULATIONS AND EXPERIMENTAL VALIDATION

D. Forcellini¹, S. Mitoulis², K. N. Kalfas³

¹ Università di San Marino
Via Salita alla Rocca, 44, 47890, San Marino
davforc@omniway.sm

² University of Surrey
Stag Hill Campus, Guildford GU2 7XH, UK
s.mitoulis@surrey.ac.uk

³ COSTAIN Engineering & Construction Limited
London Bridge Station Redevelopment, 82, St Thomas Street, London SE1 3QU, UK
kostas.kalfas@costain.com

Keywords: Earthquake Engineering, Elastomeric Bearings, Numerical simulations

Abstract. *Multi-layer elastomeric bearings are used as common means of isolation with a large number of applications over the last 20 years in infrastructure assets. In this regard, seismic isolation is one of the most promising design philosophies for protecting structures against the catastrophic effects of earthquakes. Isolated bridges should be designed to respond with minimal or no damage (i.e. essentially elastic behavior). Additionally, in isolated bridges seismically induced damage is expected to be concentrated within the isolators, which are designed to be easily replaced. Thus, isolated bridges are resilient structures as their design is aligned to the principles of resilience, i.e. low-damage and quick restoration. Elastomeric bearings can be subjected to large axial loads and /shear displacements during strong earthquakes, which may also induce buckling effects. The recent Forcellini and Kelly (2014) model for elastomeric bearings allows to take into account large deformation response of a bearing when buckling occurs.*

This paper aims to identify the accuracy of this theory using experimental results and detailed numerical simulations carried out on ABAQUS. The finite element (FE) model has been reproduced with a layered system able to represent the alternating steel and rubber layers and the bolted connections. The presented FE model can be used as a powerful tool for predicting the non-linear behaviors registered during the lab tests. This study will provide new insights useful to designers, engineers and consultants.

1 INTRODUCTION

Multi-layer elastomeric bearings have been extensively employed for pier and abutment protection against earthquakes ([1], [2], [3] and [4]). In this regard, base isolation decouples the structure from the ground by intentionally concentrating seismic energy dissipation within the isolation system. Isolated bridges are designed to respond with minimal or no damage (i.e. essentially elastic behavior). Additionally, in isolated bridges seismically induced damage is expected to be concentrated in the isolators, which are designed to be easily replaced. Generally, the bearings are used in the case of compression and somewhere in presence of shear forces. Therefore, it is necessary to have an in-depth knowledge of the behavior of such devices under these loading conditions ([5] and [6]). In this regard, elastomeric bearings can be subjected to large axial loads and lateral/shear displacements during strong earthquakes, which may also induce buckling effects. The [8] model is used to illustrate the influence of large deformations on the interaction between horizontal and vertical loads and assessing the post-buckling behavior of these bearings. In particular, the previous study was conducted with the aim to extend the original linear theory of multilayered elastomeric bearings by replacing the differential equations by the algebraic ones. The model has been recently performed in order to study some applications, [4]. In this background, this paper aims to verify this theory using experimental results and detailed numerical simulations on ABAQUS. Initially, test results are taken by the ones carried out at University of Surrey. These results have been compared with the developed theory. Secondly, numerical simulations have been performed by applying ABAQUS in order to validate both the laboratories tests and the theory. In particular, the actual state of mechanical computations allows to investigate non-linear behaviors with sophisticated numerical tools ([9] and [10]). The finite element (FE) model has been reproduced with a layered system able to represent the alternating steel and rubber layers and the bolted connections. Therefore, the paper aims to assess the theory potentialities in performing non-linear behavior of the elastomeric bearings. In particular, as shown by [11], the rotation experienced by the top and the bottom support can significantly influence the lateral behavior and cannot be neglected. In particular, the original theory has been modified in order to take into account G reduction and the rotation. The proposed modifications will be developed in order to provide new design considerations for designers, engineers and consultants all over the world.

2 CASE STUDY

In this paper, the multilayer elastomeric bearing has been taken from the ones tested experimentally at University of Surrey and numerically in recent research [7, 10] shown in Figure 1 and Table 1, where the geometry of the reference bearing is described in details.

The circular steel-laminated elastomeric bearing consists of thirty layers of a hyperelastic material with 4 mm thickness each, alternating with twenty-nine steel shims with thickness of 3.1 mm each. At the top and bottom of the isolator there are two anchor plates with 28 mm thickness each. The total thickness of the benchmark bearing is 265.9mm. The diameter of the elastomeric layers and the steel shims is 700 mm and the one of the anchor plates is 1000mm. There is a hole, at the centre of the reference bearing, with a diameter of 15mm.

The bottom anchor plate of the model is fixed. Shear displacement of 450mm and simultaneous axial pressure is imposed to the top anchor plate of the bearing. Initially, the bearing was subjected to one full cycle of shear corresponding to a shear strain of 375%, thus the shear displacement is 450 mm. Figure 2 shows the results as detailed in [6].

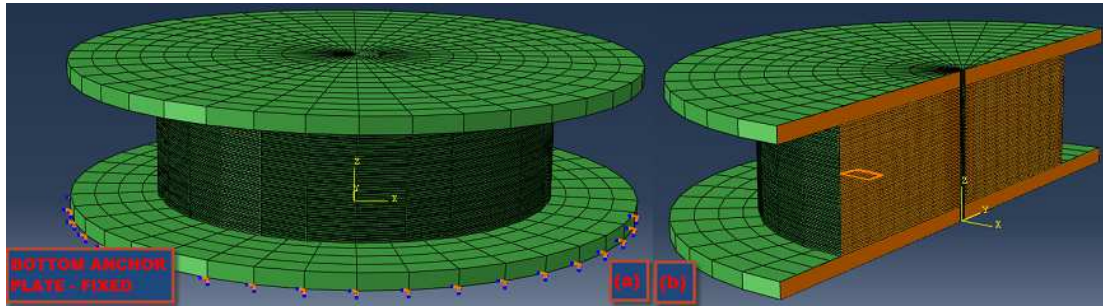


Figure 1. (a) 3D view and (b) vertical section of the benchmark steel-laminated elastomeric bearing

Table 1. Geometry of the reference bearing [7]

	notation (unit)	Value
diameter of the elastomer	D_r (mm)	700
diameter of the anchor plate	D_{AP} (mm)	1000
diameter of the hole	D_h (mm)	15
area of the elastomer layer	A_b (mm ²)	384845
total height of the bearing	T (mm)	265.9
elastomer layer thickness	t_r (mm)	4
number of elastomeric layers	n_r	30
total elastomer thickness	T_r (mm)	120
single steel shim thickness	t_s (mm)	3.1
number of steel shims	n_s	29
total steel shim thickness	T_s (mm)	89.9
single anchor plate thickness	t_{AP} (mm)	28
number of anchor plates	n_{AP}	2
total anchor plate thickness	AP (mm)	56

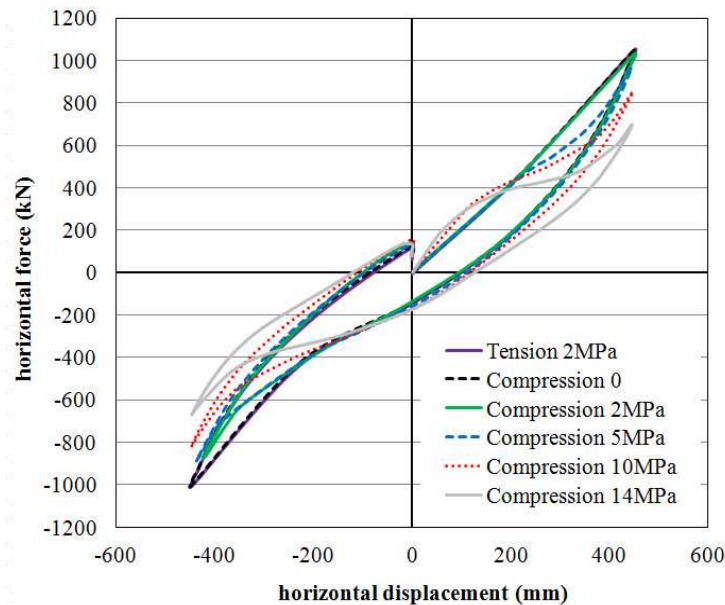


Figure 2. Response of the reference steel-laminated elastomeric bearing for variable axial loads (shear strain 375%) for one cycle of loading [7]

3 THEORETICAL MODEL

The two-spring model (shown in Fig. 3) consists of two rigid elements in the shape of tees, connected by moment springs across hinges at the top and bottom and by shear springs and frictionless rollers at mid-height, [8]. The deformation variables shown are the shear displacement (s), the relative rotation (θ) and the horizontal displacement (v). The vertical load is P while the horizontal load at the top of the column is F . The kinematic at the top of the column is thus calculated following the formulation by [8].

Fig. 4 shows the results in terms of s/h , v/h , δ/h , θ for variable values of the axial load (2MPa and 14 MPa), as calculated by the theoretical model. It is possible to see s/h and v/h are not extremely sensitive to the values of p . In particular, the axial load affects the stiffness that decreases with increasing axial load, as shown in [9].

Fig. 5 shows the shear force – displacement relationship for variable values of the axial load (2MPa and 14 MPa), as calculated by the theoretical model (red line), in relationship with the ones predicted by the numerical simulation (blue line) [7]. It is possible to see that the displacements increase linearly with the lateral shear force.

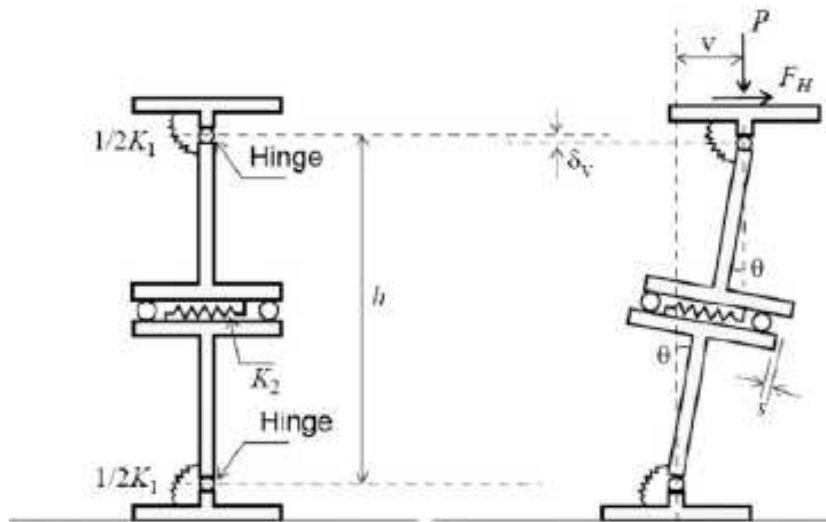


Figure 3 – Two-spring model [8]

4 SENSITIVITY ANALYSIS

In order to model the non-linear behavior, a sensitivity analysis has been performed on two important parameters. First of all, the shear modulus G in order to take into the reduction of the stiffness when the shear strain increases. The second parameter that has been studied is the top support rotation. It has been introduced in order to assess how its influence on the lateral behavior.

4.1 G modulus

G reduction when the shear strain increases has been investigated in several research, such as [12]. In this research, the model used in [13] was modified by using an instantaneous apparent shear modulus as a function of the shear strain obtained from the tests results they performed. In order to consider non-linear effects, [13] proposed a nonlinear formulation for G calibrated from the laboratory results and varying the horizontal tangential stiffness, as principal variable. In this paper, G has been varied by considering the loading conditions. In

particular, both the shear force (F) and the axial pressure (p) have been introduced inside a formulation:

$$G(p, F) = \left[1 - 0.1 \cdot \left(\frac{F}{100} \right)^{\frac{p^2}{100}} \right] \cdot G_{init} \quad (1)$$

Equation (1) leads to linear curves in cases of very low axial load (for example in case of $p = 2$ MPa). Figure 6 shows the comparison between the numerical simulation outputs (blue line, [7]), the theoretic model [8] (with constant G , in red) and the modified G (with equation 1, in green). It is shown that the theoretical approach and the numerical results improves when equation (1) is implemented inside the theory. This happens particularly in case of bigger values of p (such as 14 MPa). The model even with the formulation for considering the variation of G does not allow to consider conditions of unloading.

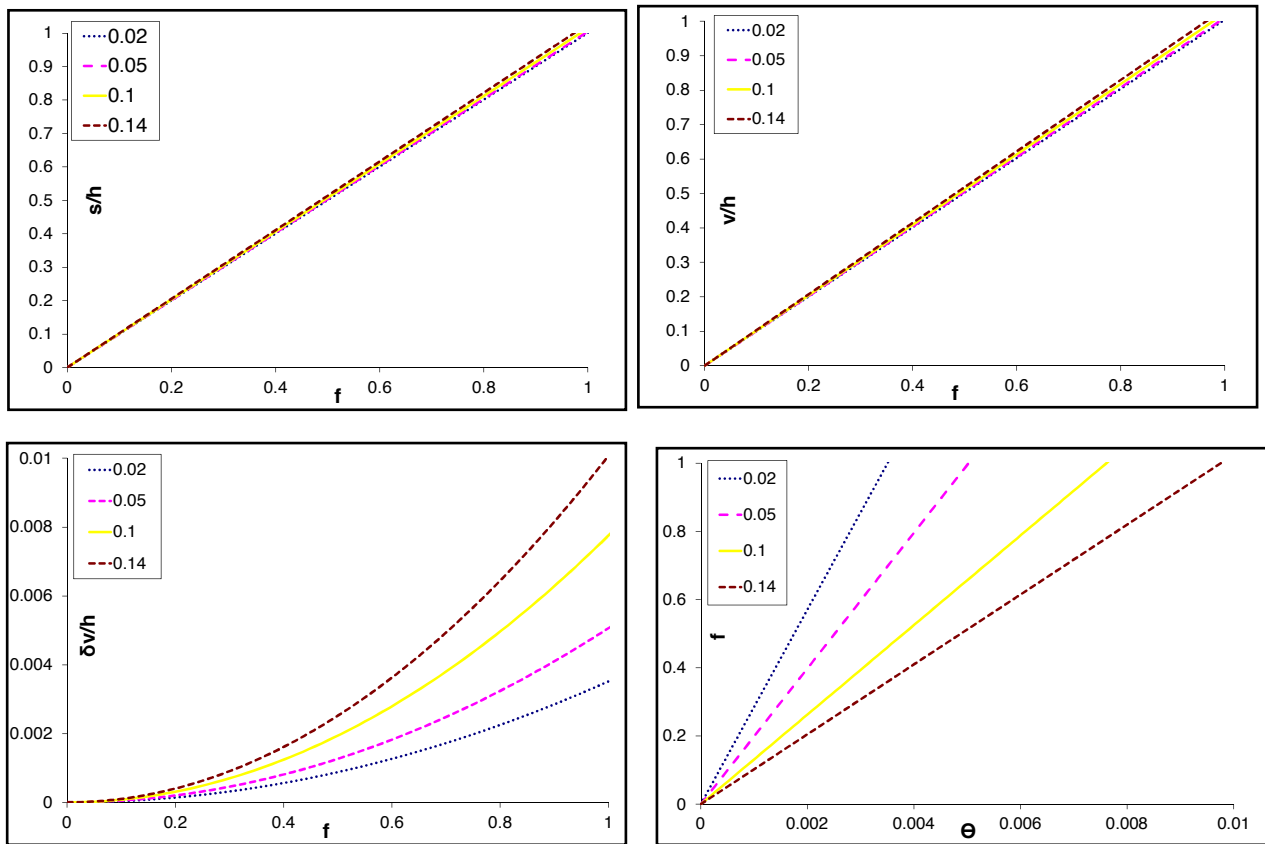


Figure 4 – Two-spring model results in terms of s/h , v/h , $\delta v/h$, θ

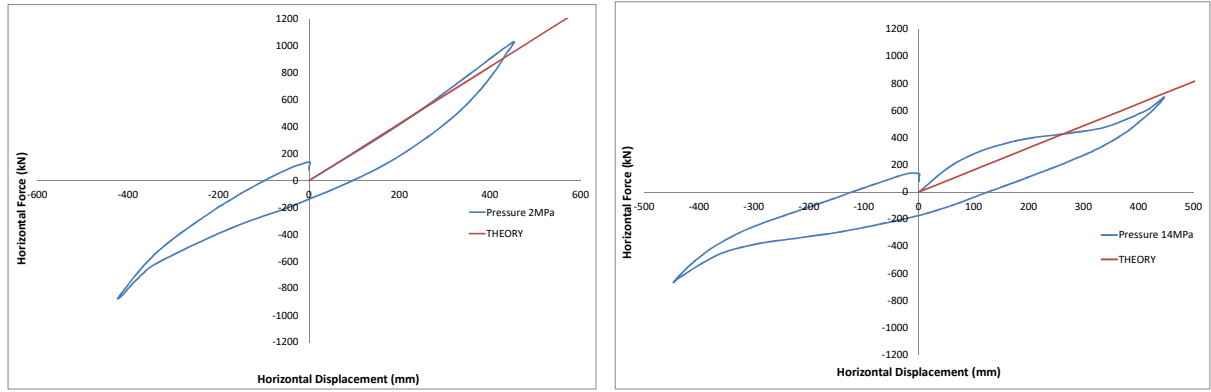


Figure 5 – Shear force-displacement curve (axial load: 2 MPa and 14 MPa [7]) following [8]

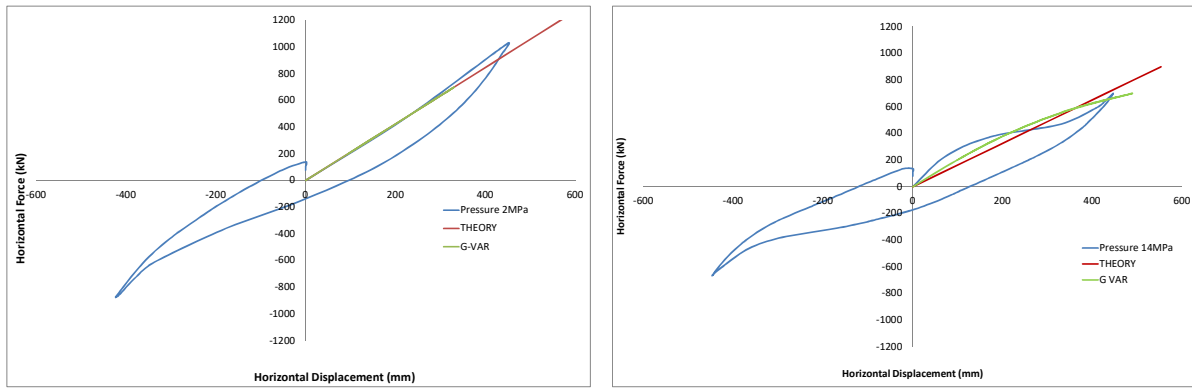


Figure 6 – Shear force-displacement: comparison between the numerical simulation outputs (blue line, [7]), the theoretic model [8] (constant G) and the modified G (with equation (1)) for axial load: 2 MPa and 14 MPa.

4.2 Rotation

Following the approach shown by [11], the rotation experienced by the top and the bottom support may influence significantly the lateral behavior and hence this should not be neglected. In this regard, the original formulation [8] has been modified by introducing the applied rotation at the top end plate (named α and positive if the same sense as θ) inside the previous formulation:

$$v = h \cdot \sin(\theta + \alpha) + s \cdot \cos(\theta + \alpha) \quad (2)$$

$$[p \cdot \cos(\theta + \alpha) + \lambda] \cdot [p \cdot \sin(\theta + \alpha) + f \cdot \cos(\theta + \alpha)] = (\theta + \alpha) \quad (3)$$

Where:

$$p = \frac{P}{\sqrt{P_E P_S}}; f = \frac{F}{\sqrt{P_E P_S}}; \lambda^2 = \frac{P_S}{P_E} \text{ (usually between 0.001 and 0.05)} \quad (4)$$

and:

$$P_E = \frac{\pi^2 \cdot E \cdot I_S}{h^2} \quad (EI_S \text{ bending stiffness}) \quad (5)$$

$$P_S = G \cdot A_s \quad (GA_s \text{ effective shear stiffness}) \quad (6)$$

Figure 7 and 8 show the effects of introducing rotation of the top support. In particular, Figure 7 shows the results when α is set to increase linearly with the horizontal shear force. Several values of initial rotation have been considered: 0.5, 1.0, 1.5 and 2.0 rad and named LIN-0.5; LIN-1; LIN-1.5; LIN-2). The results show that the first part of the curve fits with the experimental ones.

Figure 8 shows the comparison between the original theory (blue line), the previous LIN-1.5 case (black line) and the results when α is set to increase with a bi-linear behavior (red line). In particular, the red line shows that if after the plateau the rotation is maintained constant (elastic – perfectly plastic behavior), the two curves reach a proper agreement.

The model does not allow to consider conditions of unloading as well.

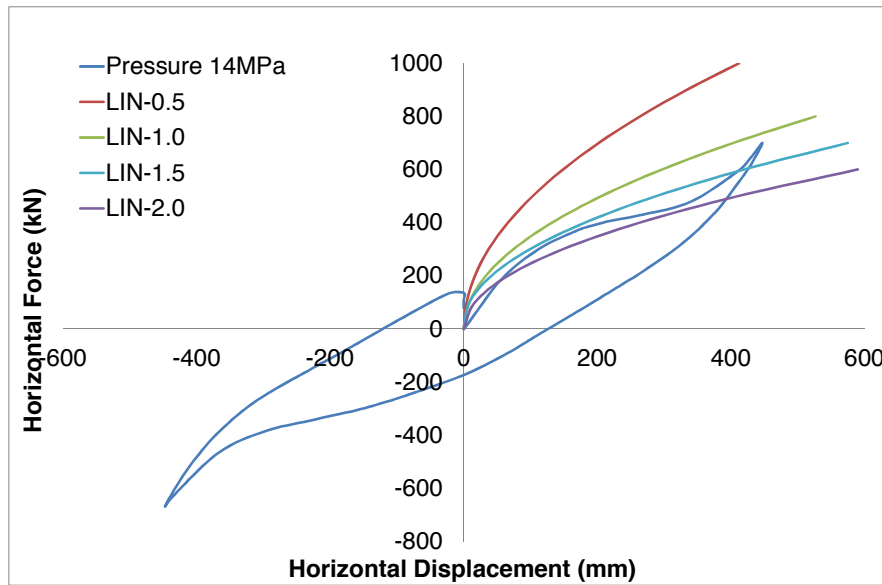


Figure 7 – Shear force-displacement curve (axial load: 14 MPa [7]): following [8] and linear rotation (initial: 0.5, 1.0, 1.5, 2.0) of top support.

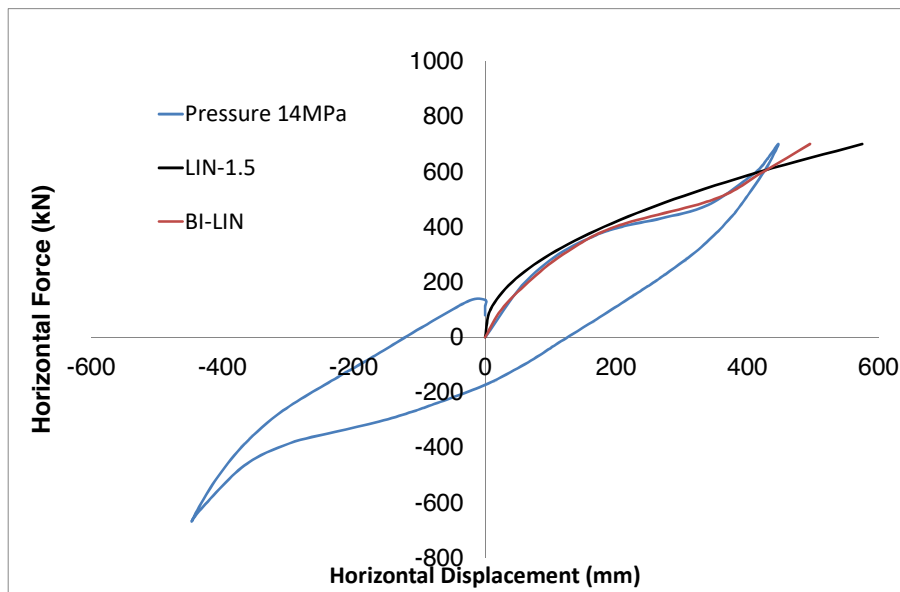


Figure 8 – Shear force-displacement curve (axial load: 14 MPa [7]): following [8], linear (initial rotation: 1.5 rad) and bilinear rotation of top support.

5 CONCLUSION

The paper aimed to apply the theoretical approach [8] in order to propose a new model able to improve the description of non-linear behaviour of the bearings. In this regard, two important parameters have been varied and implemented inside the original formulation. First, a formulation that allows to vary G has been proposed. Secondly, the effect of rotation of the supports has been considered. The non-linear behavior shown in numerical simulations [7, 10] was reproduced with two sensitivity analyses. The results show how a more developed model needs to include both the reduction of G and the effect of the rotation. Future comparisons on more bearings need to be considered.

ACKNOWLEDGEMENT

The authors want to acknowledge prof. James Marshall Kelly for his support in the implementation of the variability of modulus G and the introduction of the rotation inside the theoretical model.

REFERENCES

- [1] G.C. Manos, S.A. Mitoulis, A. Sextos *A Knowledge Based Software for the Design of the Seismic Isolation System of Bridges*. Bulletin of Earthquake Engineering, Vol. 10 (3), pp. 1029-1047, 2011
- [2] S.A. Mitoulis, *Uplift of Elastomeric Bearings in Isolated Bridges Subjected to Longitudinal Seismic Excitations*. Structure and Infrastructure Engineering, pp.1-16, 2014.
- [3] E. Tubaldi, S. Mitoulis, H. Ahmadi, A. Muhr *A parametric study on the axial behaviour of elastomeric isolators in multi-span bridges subjected to horizontal excitations*. Bulletin of Earthquake Engineering, pp.1-26. DOI: 10.1007/s10518-016-9876-9, 2016.
- [4] D. Forcellini, Cost Assessment of isolation technique applied to a benchmark bridge with soil structure interaction. Bull Earthq Eng. doi:10.1007/s10518-016-9953-0, 2017.
- [5] Q. R. Yang, et al., *Tensile Stiffness and Deformation Model of Rubber Isolators in Tension and Tension-Shear States*. Journal of Engineering Mechanics, Vol. 136, pp. 429-437, 2010.
- [6] Nguyen, H., H., Tassoulas, J., L., 2010. "Directional Effects of Shear Combined with Compression on Bridge Elastomeric Bearings". *Journal of Bridge Engineering*, Vol. 15 (1), pp. 73-80.
- [7] K. N. Kalfas, S. A. Mitoulis, K. Katakalos, 2017. "Numerical study on the response of steel-laminated elastomeric bearings subjected to variable axial loads and development of local tensile stresses". *Engineering Structures*, Vol. 134, pp. 346-357.
- [8] D. Forcellini, J.M. Kelly *Analysis of the large deformation stability of elastomeric bearings*. J Eng Mech 140(6):04014036, 2014
- [9] D. Forcellini *3D Numerical simulations of elastomeric bearings for bridges*, Innov. Infrastruct. Solut. 1:45 DOI 10.1007/s41062-016-0045-4, 2016

- [10] K. N. Kalfas, S. A. Mitoulis, K. Katakalo *Numerical study on bridge elastomeric bearings subjected to large shear strains with emphasis on local tension*. 16th World Conference on Earthquake Engineering. 9-13 January 2017, Santiago, Chile, 2017.
- [11] S. R. Moghadam, D. Kostantinidis *Modification of existing models to include the effect of rotation on the behavior of elastomeric bearings*. 16th World Conference on Earthquake Engineering. 9-13 January 2017, Santiago, Chile, 2017.
- [12] GH. Koo, JH. Lee, Yoo, B. Too, Y. Ohtori *Evaluation of laminated rubber bearings for seismic isolation using modified macro-model with parameter equations of instantaneous apparent shear modulus*. Engineering structures, 21 (7) 594-602, 1999.
- [13] CG. Koh, JM. Kelly *A simple mechanical model for elastomeric bearings used in base isolation*. International journal of Mechanical Sciences, 30 (12), 933-943, 1988.
- [14] S. Nagarajan, K. Ferrell *Stability of elastomeric seismic isolation bearings*. J. Struct. Eng. doi: 10.1061/(ASCE)07339445(1999)125:9(946),946-954, 1999